Proceedings of the Sixth IASTED International Conference
BIOMEDICAL ENGINEERING
February 13–15, 2008, Innsbruck, Austria
ISBN Hardcopy: 978-0-88986-721-5 / CD: 978-0-88986-722-2

MODELLING AND MEASUREMENT OF ODOUR TRANSPORTATION WITHIN THE HUMAN NASAL CAVITY

J. W. Gardner, S. Nadarajan and P. Kimber
Centre for Cognitive & Neural Systems
School of Engineering, University of Warwick, Coventry, CV4 7AL, UK
Email: j.w.gardner@warwick.ac.uk

ABSTRACT
Human breathing behaviour varies from quiet breathing to forceful sniffing but can, in general, be modelled as turbulent airflow. Here an anatomically correct, 3-D model of the human nasal cavity has been created using 3D CAD software and manufactured using rapid prototyping technology. Firstly, the CAD model is used to simulate the flow of an odour through the nasal cavity using computational fluid dynamics (CFD). CFD is used to predict the velocity field within the adult nasal cavity by solving numerically the set of governing Navier-Stokes equations. The effect of nasal cavity size upon the flow fields of sniffing was also investigated. Second, chemo-resistive odour sensors were implanted within the nares; superior, medial and inferior concha or turbinates; and nasopharynx of a 3-D model of the nasal cavity. These sensors were able to detect the concentration of an odour as it travels within the nasal cavity and at the olfactory mucosa (top of superior turbinate). Our experimental measurements agreed with the computer simulations and demonstrate that a small proportion of the odour is transported to the olfactory mucosa and that it is comparatively stagnant. We believe that by modelling the flow of odours within the human nasal cavity we will be able to design a superior generation of electronic noses for medical diagnostics.

KEY WORDS
Modelling, biomechanics, artificial olfaction

1. Introduction

Olfaction is one of the five senses originally described by Aristotle but perhaps the most difficult to understand. Some 100 million specialised receptor cells located within human olfactory epithelium detect the presence of odorant compounds. The olfactory epithelium and receptor cells (i.e. mucosa) are located at the top of the superior concha in each of the two nasal cavities within the human nose, as shown in figure 1. The odorant must possess certain molecular properties in order to provide sensory properties, such as aqueous solubility. The dissolved molecules interact with receptors on cilia to create an electrical spiking signal that is transmitted to the olfactory bulbs and higher brain via glomeruli nodes and mitral cells. In this way, our biological nose detects the presence of odorous compounds in air [1].

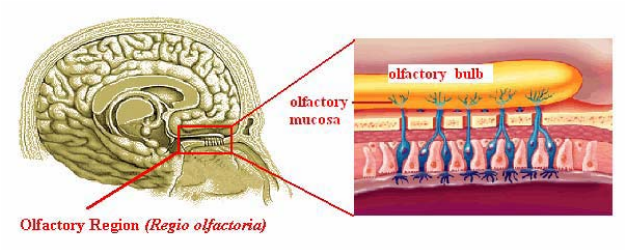

Figure 1 Diagram showing the location of the olfactory region and the olfactory epithelium [2,3]

According to recent Nobel Prize winner in olfaction, Linda Buck, these nerve signals reach defined micro regions in the brain cortex, where the information from several types of odorant receptors is combined into a pattern characteristic for each odour [4].

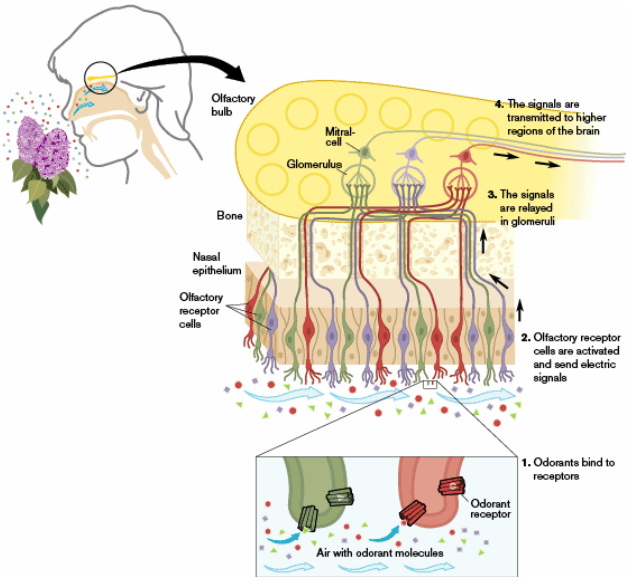

Figure 2 Diagram showing the olfactory system

This information is then interpreted and leads to the conscious experience of a recognizable odour. Figure 2 shows the odorant receptors and the general organization of the olfactory system (also see refs [1] and [4]).

Our research is directed towards the general field of artificial olfaction and electronic noses. Here we have focussed our study to the movement of odours within the human nasal cavity and, especially, to the region of the olfactory mucosa. The main purpose of this study is to obtain numerical simulations of flow fields over a range of conditions from quiet breathing to forceful sniffing and then compare these with measured values in a 3-D artificial nose.

A model of the human nasal cavity was obtained and implemented within the commercial software package of SolidWorks™. Computational Fluid Dynamics (CFD) was used to determine the theoretical flow of odours through the nasal cavity with the toolbox of COSMOSFloWorks™. Previous studies have been made to compute the flow patterns in the nasal cavity because of interest in dysfunctional noses [5]. However, our work is different in that we have not only investigated the affect of nose size on flow patterns but also, and more importantly, related this to the field of artificial olfaction. This has been done by constructing a 3-D prototype nose based upon a normal male adult nose.

2. Method and set-up

Our experimental work can be divided into two sections. The first section describes the computer simulation of the human nasal cavity using the computational fluid dynamic (CFD) approach. The second section describes the construction and testing of a 3-D model with embedded odour sensors.

2.1 Computational nasal flow patterns

The commercial package SolidWorks™, with its toolbox of COSMOSFloWorks™, was used to build the anatomically correct right nasal cavity and to carry out the simulations based upon solving the Navier-Stokes equations for turbulent fluid flow.

The nasal model was obtained by CT imaging from a 25-year-old healthy male. The geometry of the nasal cavity was reconstructed as a 3-D CAD model and imported into SolidWorks™. SolidWorks™ is a 3-D CAD (computer-aided design) program that runs on a PC under Microsoft Windows and was developed by SolidWorks Corporation, which is now a subsidiary of Dassault Systèmes (France). The contours of the right nasal cavity were manually digitised for each cross section on twenty-nine different sections, which were based on the structures shown in figure 3. The number on each section represents the distance of each planar section from the previous section. The cross-sections shown are taken from the work of Kelly et al. [5].

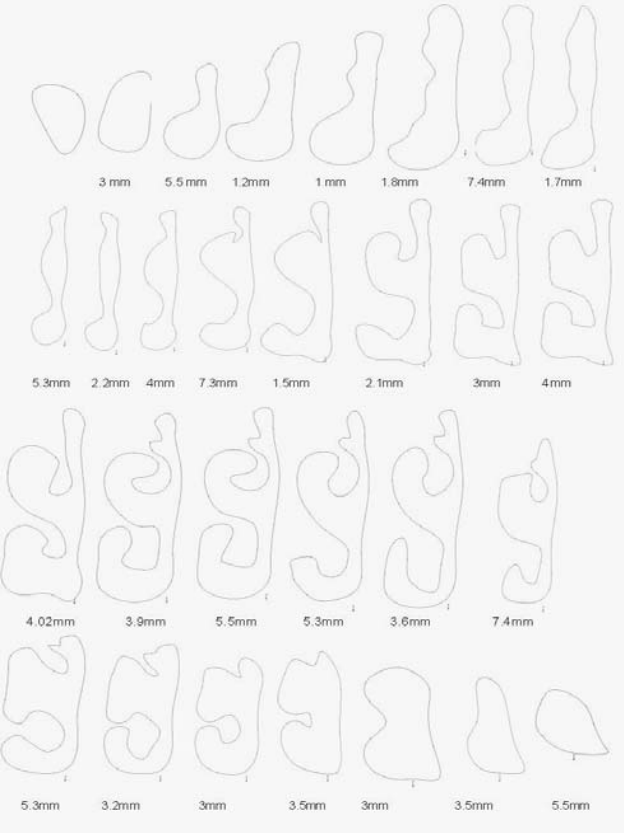

Figure 3 Coronal computed tomography scan based on Kelly et al. Numbers indicate the distance in mm from the previous cross section

Once all the sections were digitised, they were lofted together using a SolidWorks™ feature that digitally links together each cross-sectional plane. The software effectively catenates material in between the sections to create the solid model shown in figure 4.

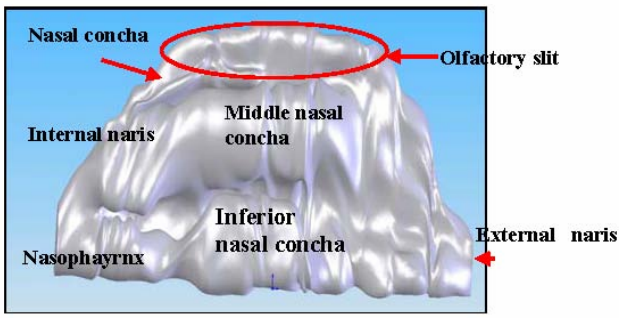

Figure 4 Solid model of the human nasal cavity that was constructed using SolidWorks™ with labels showing key biological regions

Similarly, seven other nasal cavity models were constructed and modelled with the details given below in Table 1. Once the modelling was completed, computer simulations were carried out using COSMOSFloWorks™. COSMOSFloWorks™ was chosen for these simulations because it offers fully automated mesh generation of complex geometries with local adaptive refinement,

automated handling of laminar, turbulent and transitional flow regimes within one model based on an enhanced two- equation turbulence model of the k-e type.

There were several boundary conditions that were applied besides the inlet and the outlet conditions mentioned above. They are; pressure applied of 101,325 Pa, temperature applied of 293.3 K, has slight turbulence intensity of 2% and a turbulence length of 0.345 mm.

The flow through the nasal cavity was pure dry airflow, steady-state, incompressible, and isothermal. Simulations were carried out at volumetric flow rates of 50 mls-1, 100 mls-1, 125 mls-1, 200 mls-1, 300 mls-1, 400 mls-1, 500 mls-1 and 600mls-1. These values range from the equivalent of gentle breathing to strong sniffing.

2.2 Experimental set-up

A fused deposition modeller (Stratasys Inc. Dimension BST 768) was used to create a positive model of the cavity in ABS (acrylonitrile butadiene styrene) from the 3D CAD model. Cores for each of the sensors and airway connections were added to the cavity model before it was encased in cold curing silicon rubber compound. After curing, the ABS positive model was removed, leaving the cavity within the white rectangular block of silicon rubber visible in figure 5. Odours are injected into the inlet of the block using a syringe (BD Plastipak, 1 ml) and drawn through the model using a variable electrical pump (Charles Austin Pumps Ltd, Model F75 SE). The volumetric flow rate was measured using a manometer.

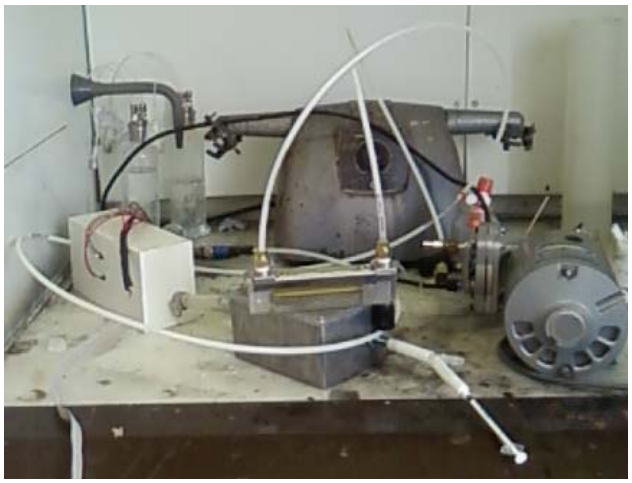

Figure 5 Experimental arrangement used to measure the odour pulses within the artificial nasal cavity

Six identical odour sensors have been made and they consist of a polymer/carbon composite film deposited on top of interdigitated gold electrodes on a passivated silicon substrate. The 2 mm by 2 mm silicon die is then mounted and wire bonded onto a TO-5 header for insertion into the model. Full details of this type of odour sensor can be found in reference [6]. The resistance of the odour sensors was measured using a current source (Knick, DC calibrator J152) set to a value of 2.5 mA and a digital oscilloscope provided time series traces.

The odour sensors were placed inside the nasal cavity at six different locations including the olfactory epithelium. The sensors were positioned flush with the cavity walls to minimise disruption to fluid flowing around the sensors.

Table 1
Details of the eight different geometrical shapes of the nasal cavity modelled using computational fluid dynamics

Shape number and description
Shape 1- Original Size with the length of the nose being 107.22 mm
Shape 2- Original size with shorter plane length with the length of the nose being 99.82 mm
Shape 3- Length of olfactory is longer than the original size and has same a plane length with the length of the nose being 106.82 mm
Shape 4- Length of olfactory is longer than the original length size and has a longer plane length with the length of the nose being 112. 92 mm.
Shape 5- Length of olfactory is shorter than the original size and has a longer plane length with the length of the nose being 112.42 mm.
Shape 6- Original olfactory size and has a longer plane length with the length of the nose being 104.72 mm.
Shape 7- Length of olfactory is shorter than the original size and has same a plane length with the length of the nose being 107.22 mm.
Shape 8- Length of olfactory is shorter than the original size and has a shorter plane length with the length of the nose being 103.52 mm.

Figure 6 shows a close-up photograph of the nasal cavity model with the wires connected to the embedded sensors clearly visible. The odours are then injected into the flow stream and the signals recorded at various positions inside the nasal cavity. The dc electrical resistance of the polymer/carbon black composite sensor increases when the odour is present and the increase is proportional to the concentration of odour in air.

Figure 6 Photograph of 3-D model of nasal cavity with six embedded odour sensors

3. Experimental results

Our experimental results can be divided into two parts:

- The theoretical airflow patterns expected inside our 3-D model of the nasal cavity
- The odour concentration measured inside our solid model of the nasal cavity

Simulations were obtained for the eight different shapes of nasal cavities described in table 1. Results of the airflow patterns are shown in figures 7 and 8.

The velocity trajectories transecting the nasal passage flow are shown in figure 7. This figure illustrates the airflow distribution within the nasal cavity. The colours represent zones of low velocity 1 m/s (blue) through to high velocity of 8.85 ms-1 (red) and hence velocity map the nasal region. The flow distribution becomes weaker at the wide exit of the nose (left-hand side). It can also be observed that the olfactory slit (superior conchra) has the lowest velocity, which appears almost stagnant.

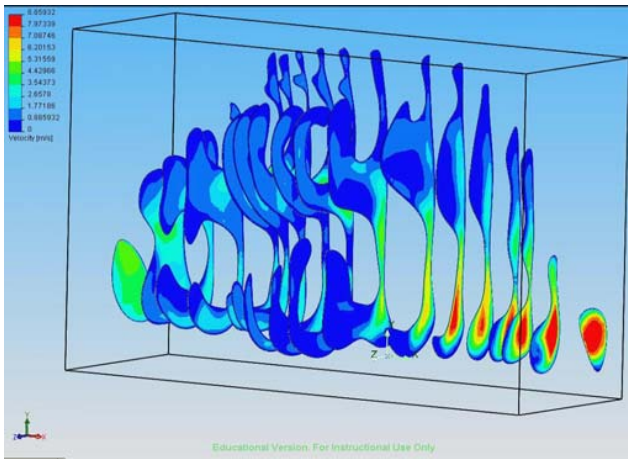

Figure 7 Air flow distribution inside the nasal cavity

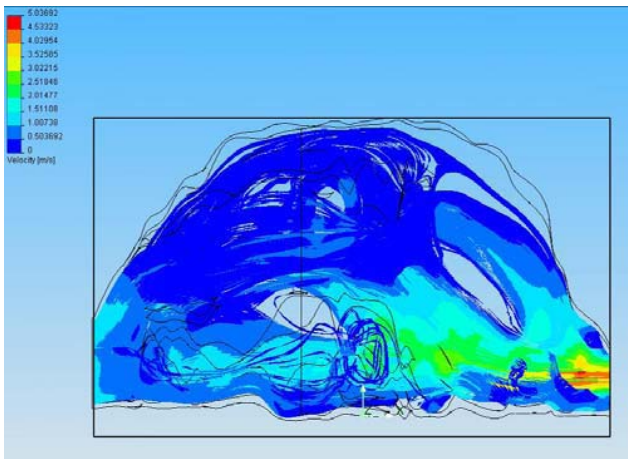

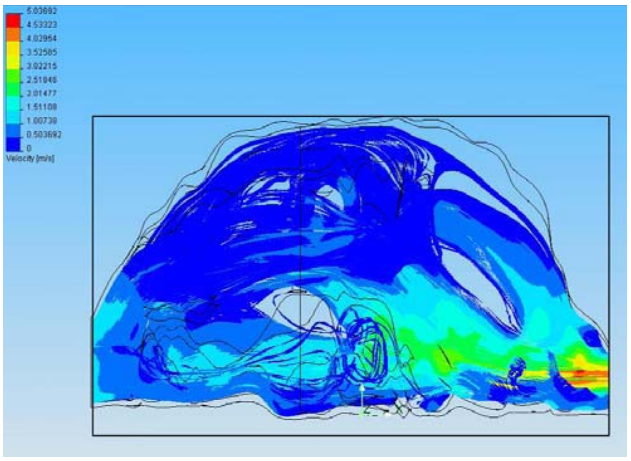

Figures 8(a) and 8(b) shows the difference between the flow patterns within two different sizes of nasal cavity at a volumetric flow-rate of 200ml/s

Figures 8(a) and 8(b) show an example of the comparison of recorded flow trajectory at a volume flow rate at 200 ml/s. The comparison is carried out between nasal cavity shape 1 and nasal cavity shape 5. It is shown that at 200 ml/s, shape 1(a) has a lower velocity compared to shape 5.

Figure 9 illustrates the effect of the length of the nasal cavity upon the velocity. The four nasal shapes labelled 2, 7, 8 and 5 have shorter cavities compared with nasal shapes 4, 6 and 3. It is also evident that there is a rise in the gradient at a volumetric flow-rate of 0.0004 m3/s (400 ml/s), which is known as the forceful sniff, and upwards. It can also be seen, as expected, that the velocity at the olfactory bulb is low when the volume flow rate is low, which is known as quiet breathing.

From these patterns it is concluded that the velocity varies considerably in different nasal cavity sizes at constant flow rate, see Figure 9. However in the human body there will be scaling between the size of the nose and the lungs so this should reduce this effect in practice. In general the smell of a material is not a strong function of sniff velocity and so we can assume that the olfactory signal processing is weakly velocity dependent.

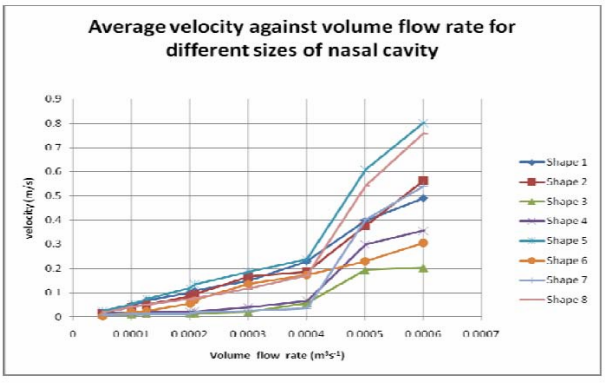

Figure 9 Plot of velocity against volumetric flow rate for different shapes of the nasal cavity at the olfactory epithelium

As has been shown elsewhere, there can be a gas chromatographic effect in the olfactory mucosa [7]. This suggests that the human olfactory system learns from differential delays and not absolute values of flow velocities.

Once the simulation and results obtained were completed, an odour (ethanol) of 0.1 ml was passed through the block nose as shown below. Once the odour reaches the sensors the digital oscilloscope detects it and there will be a rise in the graph as shown in figure 10. In this case sensor 4, which is located at the centre of the olfactory slit, is being monitored. Because of the reduced odour concentration at this point the signal is quite noisy.

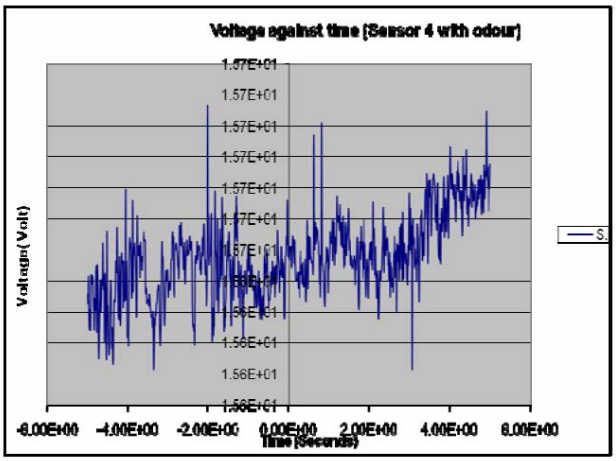

Figure 10 Voltage against time with the presence of odour

Sensor 4 is placed at the middle of the olfactory slit which is roughly around 56.32 mm. By integrating the velocity obtained using the range of volume flow rate, the time taken for the odour to travel from the naris to olfactory slit in different nasal shapes can be calculated. These are shown in table 2.

Table 2
Shows the volume flow rate and the time delayed for the odour to reach the sensors

Volume flow rate (ml/s)	Average velocity (m/s)	Time delayed (s)
50	0.01868	3.3697
100	0.04747	3.2362
125	0.06730	3.1146
200	0.09966	2.7890
208§	0.10869	2.3967
300	0.15006	1.4040
400	0.22966	0.8451
500	0.39679	0.1885
600	0.49038	0.1583

§This value was added to compare with the work of Weinhold et al.

4. Conclusion

We have created a 3-D solid model of the human nasal cavity based upon the nose of a healthy 25 year old male adult. We then analysed the flow patterns through this nasal cavity and others using both a systematic variation in the dimensions as well as flow-rates ranging from gentle breathing to forceful sniffing. The flow patterns produced suggested that most of the odour bypasses the olfactory slit and that the flow velocities are much lower in this region. Next we constructed a 3-D model of the nasal cavity and implanted sensors to measure the flow velocities directly. We were also able to calculate the delay times for the odour to reach the olfactory epithelium and these can be fractions of a second.

Our model of the nasal cavity is still rather basic. First the surface of the cavity will influence the flow patterns and odour transport along its length. In addition, there is some evidence elsewhere that the hairs inside the nostrils help mix the air flow and hence make the flow pattern even more turbulent. Nevertheless we believe that this is the first time a model of the nasal cavity has been built and a study carried out of the transportation of an odour from the naris to the olfactory mucosa.

One of our primary reasons for studying the airflow inside the nasal cavity was the belief that it will help us design a new generation of electronic noses that more closely mimic the biological system. Existing electronic noses do not yet have the sensing capability of the human nose and so further research effort is required to achieve that end goal. A particular interest of ours is to use an electronic nose to detect infectious diseases, which has shown some promising early results [8].

A secondary reason for this research is that it may help to find an alternative method for delivering drugs by nasal injection as illustrated in figure 11.

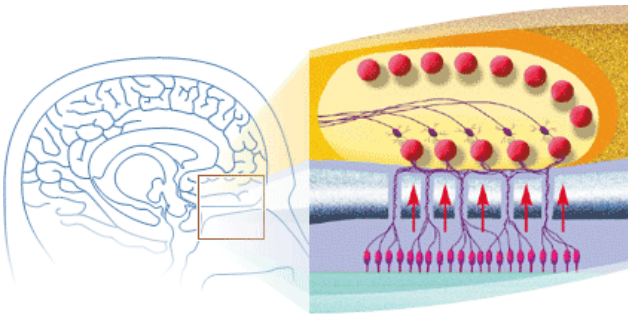

Figure 11 Direct to brain delivery of intranasal drugs may be facilitated by the incomplete blood-brain-barrier in the olfactory region

There are several potential advantages of nasal delivery such as [9]:

- Ability to deliver a wide range of therapeutics
- Non-invasive method compared to injections
- Rapid onset of action critical to some disease states, such as immediate pain relief

- Avoidance of first-pass hepatic metabolism that consumes a drug before it has a chance to work
- Potential for direct delivery to the brain

For these reasons we feel that studying the fluid mechanics of the nose is an important issue and has been somewhat overlooked in the past.

Acknowledgements

We wish to thank Mr. Frank Courtney (Warwick University) for his technical support and Mr Boris Kirov (School of Engineering) for his initial study on an MSc project.

References

[1] J.W. Gardner and P.N. Bartlett, Electronic Nose: principles and application (Oxford, Oxford University Press, 1999).
[2] From http://www.leffingwell.com/olfaction.htm
[3] From http://www.morphonix.com/software/education/science/brain/game/specimens/olfactory_bulb.gif
[4] From http://nobelprize.org/nobel_prizes/medicine/laureates/2004/press.html
[5] J.T. Kelly, A.K. Prasad, & A.S. Wexler, Detailed flow patterns in the nasal cavity, American Physiological Society, 2000, 323-337.
[6] S.L. Tan, J.A. Covington, & J.W. Gardner, Velocity-optimised diffusion for ultra-fast polymer-based resistive gas sensors, IEE Proc. Sci. Meas. Technol., 153, 2006, 94-100.
[7] J.A. Covington, J.W. Gardner, A. Hamilton, T.C. Pearce, & S.L. Tan SL, Towards a truly biomimetic olfactory microsystem: an artificial olfactory mucosa, IET Proc. Nanobiotechnology, 1, 2007, 15-21.
[8] R. Dutta, D. Morgan, N. Baker, J.W. Gardner, & E.L. Hines, Identification of Staphylococcus aureus infections in hospital environment: electronic nose based approach, Sensors and Actuators B, 109, 2005, 355-352
[9] From http://www.nastech.com/nastech/nasal